Very Large Floating Structure (VLFS) interacting with water waves: large scale laboratory experiments and numerical modelling

Alan Tassin[a], Vincent Cognet[a], Antonin Eddi[b], Marc Fermigier[b]
a. IFREMER, RDT, F-29280 Plouzané, France
b. PMMH, CNRS, ESPCI Paris, Université PSL, Sorbonne Université, Université de Paris, Paris, France
Email: alan.tassin@ifremer.fr

1 Introduction

Domino et al. (2018) investigated experimentally the propagation of hydroelastic waves in a small water tank (80 cm×40 cm×20 cm) covered by a thin elastic plate. They showed that it was possible to control the refraction angle of the hydroelastic waves at the interface between two regions of different flexural stiffness independently of the wavelength in the purely hydroelastic regime, *i.e.* when $gk >> (D/\rho)k^5$ (g, k, D and ρ being the acceleration of gravity, the wave number, the flexural modulus of the plate and the fluid density, respectively). They also demonstrated that it was possible to focus/defocus waves over a large bandwidth using this property. We now investigate experimentally and numerically the interaction between water waves and a very large floating structure. We also aim at demonstrating at larger scale the feasibility of a "hydroelastic lens" for the focusing of water waves. Two experimental campaigns were conducted in a large wave tank with a large lightweight floating structure. The first one was conducted with a 16.25m by 4.9m rectangular plate in order to validate our ability to generate hydroelastic waves in a wave tank and to validate a numerical hydroelastic model. In the second campaign, a hydroelastic focusing lens was added at the end of the plate to study the efficiency of such a device.

2 Experimental set-up

The first experimental set-up described in figure 1 consisted in a large rectangular plate anchored at the centre of the wave tank by three aerial mooring lines (two in the front and one in the back), see figure 1(c) (top view). The plate was composed of 7 pieces made out of a 2.5 cm polyester glass-fibre sandwich material which were screwed to each other (see figure 1(c), side view). The nominal flexural modulus of the plate was 3000 N.m, but some local reinforcements were added at the junctions. Overall, the longitudinal lineic mass was approximately equal to 65 kg/m. Some lightweight expanded foam was added in the periphery of each plate in order to avoid wave overtopping, but their contribution to the global stiffness was negligible. For the second experimental campaign, the last two pieces of the plate were replaced by a focusing lens composed of two pieces forming a parabolic lens, as depicted in figure 2. Inside the parabolic contour represented in black the bending modulus was increased to approximately 10000 N.m. This increase in the stiffness leads to an increase of the celerity of the hydroelastic waves locally, and therefore the water waves are focused 1 to 2 m downstream of the lens. The deflection of the plate was recorded using spherical tracking markers distributed along 5 lines (L_1 to L_5) and a Qualysis optical tracking system composed of 8 video cameras distributed on both sides

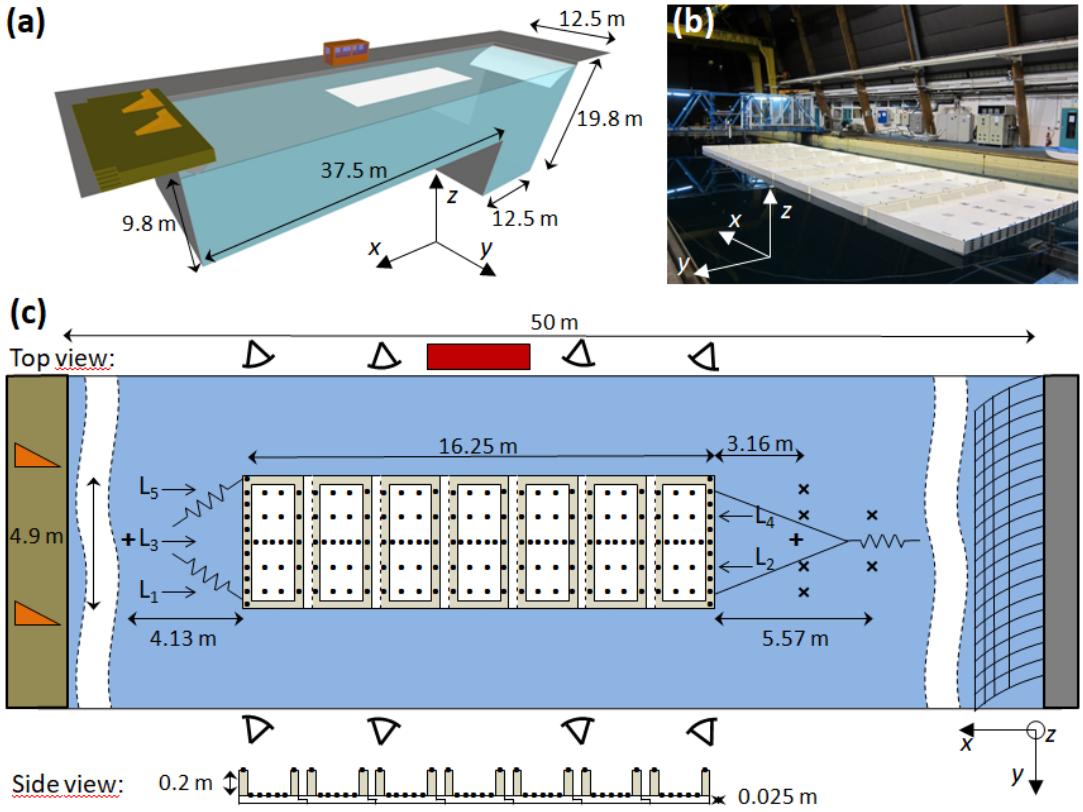

Figure 1: Description of the first experimental set-up with a rectangular plate (a) Three-dimensional sketch of IFREMER's deep water wave tank in Plouzané, France. The waves travel from the wave generator (green) on the left to the damping beach (white) on the right. The white flexible structure is in the center. (b) Picture of the flexible structure in the wave tank. (c) Top view and side view of the structure with dimensions, mooring lines with their springs, and location of the markers (black full circles), the probes ('+' and '×' crosses), and the eight cameras. L_1, L_2, L_4 and L_5 are lines of 28 markers along the x-axis, line L_3 have 49 markers along the x-axis.

of the tank (see figure 1(c), top view). The wave field was characterized by two servo-controlled wave gauges upstream and downstream of the plate ("+" sign in figure 1(c), top view) and six capacitive wave gauges downstream ("×" sign in figure 1(c), top view). We studied the interaction between the plate and incoming waves in both regular and irregular unidirectional waves conditions.

3 Numerical modelling

The experiments with the rectangular plate were reproduced numerically with a linear hydro-elastic model. In this model, the vertical deflection of the plate, $W(x,t)$, was assumed to be uniform in the transversal y-direction and to be governed by the Euler beam equation:

$$D\frac{\partial^4 W}{\partial x^4} - m_b\frac{\partial^2 W}{\partial t^2} - p(x,t) = 0, \tag{1}$$

where D is the flexural modulus of the plate, m_b the surfacic mass and p is the pressure exerted by the water on the plate. Equation 1 was solved in the frequency domain using

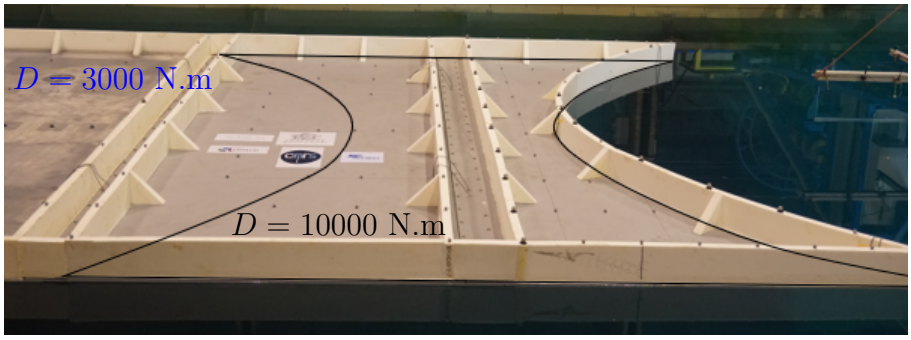

Figure 2: Picture of the focusing parabolic lens defined by $x = \pm(0.8 + y^2/4)$ m

a standard normal-mode approach with the deflection decomposed as follows:

$$W(x,t) = \Re\left(\sum_{n=1}^{N}\sum_{m=1}^{M} w_{n,m}\psi_n(x)e^{j\Omega_m t}\right), \tag{2}$$

where functions ψ_n are the mode shapes of a free-free beam in vacuum and coefficients $w_{n,m}$ are the (complex) amplitudes of the different modes at the different frequencies Ω_m. Note that the action of the springs on the vertical deflection of the plate was neglected in the model. Assuming that the pressure derives from a linear radiation-diffraction approach and following the normal-mode approach, the amplitude of the different modes can be found by solving the following equation:

$$\{-(\mathbf{M} + \mathbf{M_a})\Omega_m^2 + j\mathbf{B}\Omega_m + (\mathbf{K_e} + \mathbf{K_{hs}})\}\vec{w}_m = \vec{F}_{exc}, \tag{3}$$

where $\vec{w}_m = (w_{1,m}, ..., w_{N,m})^\intercal$, $\mathbf{M}$ is the mass matrix, $\mathbf{M_a}$ is the added-mass matrix, $\mathbf{B}$ is the wave damping matrix, $\mathbf{K_e}$ is the elastic stiffness matrix, $\mathbf{K_{hs}}$ is the hydrostatic stiffness matrix and $\vec{F}_{exc}$ is the wave excitation force vector. All the hydrodynamic coefficients ($\mathbf{M_a}$, $\mathbf{B}$, $\vec{F}_{exc}$) were computed using *Hydrostar*©. In these computations, the three-dimensional flow around the plate was computed with different boundary conditions: with and without the side walls of the tank.

4 Results

Let us first compare the dispersion relation (in the plate) obtained from the experiments and the numerical simulations with the linear surface gravity wave dispersion relation and the two-dimensional linear hydroelastic dispersion relation. The results obtained from the different approaches are depicted in figure 3. One can see that the flexural modulus of the plate is sufficiently large to modify the dispersion relation over a rather large frequency bandwidth. The dispersion relation obtained numerically and experimentally differ slightly from the theoretical hydroelastic dispersion relation, $\omega^2 = gk + (D/\rho)k^5$, probably because of the finite size of the plate. Indeed, note that the wave length in the plate is larger than the width of the plate for $T > 1.1$s. The experimental results obtained from the regular and the irregular waves are close to each other. Note however that the irregular wave results display some irregularities and that the results "oscillate" around the numerical results obtained "without walls". The numerical results obtained with the tank walls follow a very similar trend as the irregular wave experimental results, which

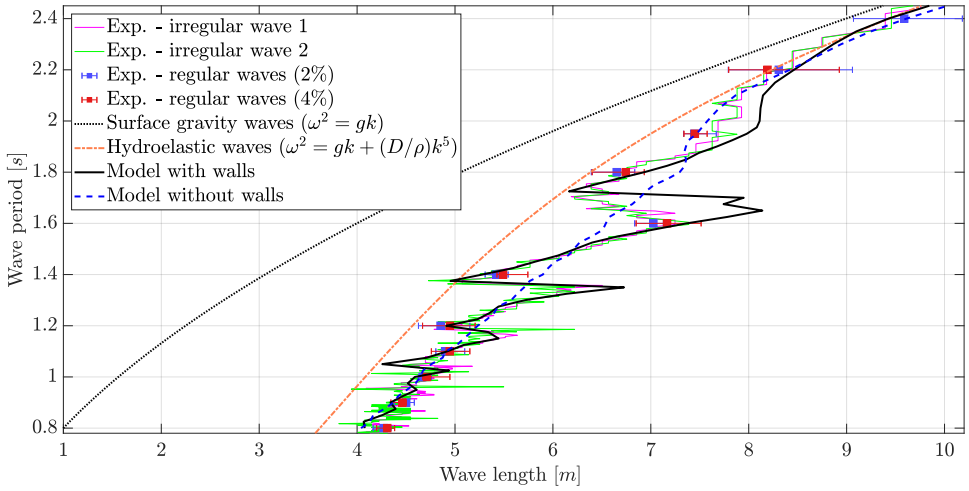

Figure 3: Evolution of the wave period in the plate as a function of the wave length.

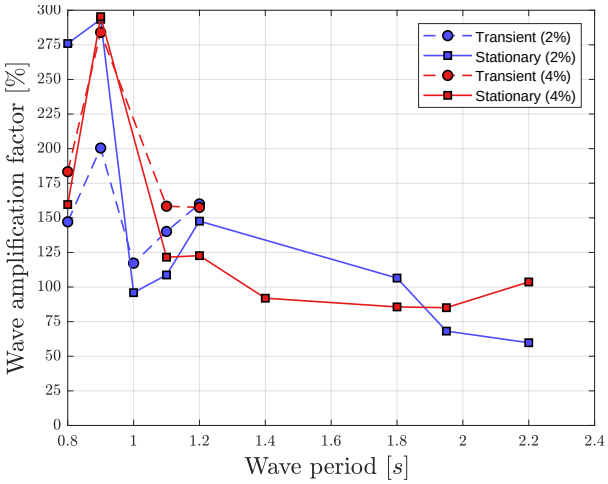

Figure 4: Evolution of the wave amplification factor as a function of the wave period.

shows that the walls of the tank affect the experiments (certainly because of the high blockage ratio). The overall agreement between the experiments and the numerical model is very good. More results have been obtained (*e.g.* amplitude of the deflection) and will be presented in more details at the workshop. Let us now observe the amplification of the wave elevation obtained with the focusing lens behind the plate. The amplification factor depicted in figure 4 corresponds to the ratio between the wave elevation behind the focusing lens and the wave elevation behind the rectangular plate. Note that, for the short waves, a distinction is made between the early transient stage and the later stationary regime because, after a certain time, the incoming waves which travel on the sides of the plate arrive at the rear of the plate and are refracted towards the wave gauge. This increases "artificially" the amplification factor in the stationary regime. Note that a significant amplification is obtained for the short waves, *i.e.* in the hydroelastic regime.

References

Domino, L., Fermigier, M., Fort, E. & Eddi, A. (2018), 'Dispersion-free control of hydroelastic waves down to sub-wavelength scale', *Europhysics Letters* **121**(1), 14001.